

K, especially in view of the fact that the antimony compounds we are concerned with in this Letter are not polymers.<sup>8</sup> Furthermore the two values of  $\epsilon$  thus deduced differ considerably, which reveals the weakness of the GKE analysis.

(4) We notice that the quadrupole coupling constant yielded by the TI analysis is smaller by about 3% than that obtained from a SOL analysis (Table I). The TI value for  $e^2q_zQ$  at 77 K is  $-20.89(40)$  mm/sec. With the usual temperature dependence of  $e^2q_zQ$  observed in such compounds, these results are in good agreement with the nuclear-quadrupole-resonance value of 20.02 mm/sec reported at 300 K.<sup>9</sup> The ratio of the nuclear quadrupole moments of the  $\frac{7}{2}$  and the  $\frac{5}{2}$  levels in  $^{121}\text{Sb}$  agrees well with the previous determination  $(1.34 \pm 0.01)$ .<sup>2</sup>

In conclusion we would like to express our concern regarding the analysis of Mössbauer spectra without accounting for  $T_A$  when the components are unresolved. In addition to  $^{121}\text{Sb}$ , similar situations also arise in  $^{127}\text{I}$  and  $^{151}\text{Eu}$ . An analysis to correct for the exponential absorption would help to report more reliable hyperfine interaction parameters<sup>12</sup> and avoid predicting physically unreasonable effects.

We thank Ludmann-Obier for providing us with the samples.

<sup>1</sup>V. I. Goldanskii, E. F. Makarov, and V. V. Khrapov, *Phys. Lett.* **3**, 344 (1963); S. V. Kariagin, *Dokl. Akad. Nauk SSSR* **148**, 1102 (1963); I. P. Suzdalev and E. F. Makarov, in *Proceedings of the Conference on the Application of the Mössbauer Effect, Tihany, Hungary, June 1969*, edited by I. Dézsi (Akademiai Kiado, Budapest, 1971), p. 201.

<sup>2</sup>J. G. Stevens and S. L. Ruby, *Phys. Lett.* **32A**, 91 (1970).

<sup>3</sup>S. Margulies and J. R. Ehrman, *Nucl. Instrum. Methods* **12**, 131 (1961).

<sup>4</sup>J. G. Stevens and L. H. Bowen, in *Mössbauer Effect Methodology*, edited by I. J. Gruverman (Plenum, New York, 1970), Vol. 5, p. 27; G. G. Long, J. G. Stevens, R. J. Tullbane, and L. H. Bowen, *J. Amer. Chem. Soc.* **92**, 4230 (1970).

<sup>5</sup>M. Pasternak and T. Sonnino, *J. Chem. Phys.* **48**, 2004 (1968).

<sup>6</sup>G. K. Shenoy and J. M. Friedt, to be published.

<sup>7</sup>H. D. Pfannes and U. Gonser, *Appl. Phys.* **1**, 93 (1973).

<sup>8</sup>R. H. Herber and S. Chandra, *J. Chem. Phys.* **52**, 6045 (1970).

<sup>9</sup>T. B. Brill and G. G. Long, *Inorg. Chem.* **9**, 1980 (1970).

<sup>10</sup>It appears that in a similar analysis in Ref. 2, different angular distributions of the  $\Delta m=0$  transitions were not considered.

<sup>11</sup>The time required for the fitting is of the order of 15 min for a spectrum with 200 data points.

<sup>12</sup>E. Gerdau, W. R  th, and H. Winkler, *Z. Phys.* **257**, 29 (1972).

## Observation of Self-Steepening of Optical Pulses with Possible Shock Formation

D. Grischkowsky,\* Eric Courtens,† and J. A. Armstrong\*

*IBM Thomas J. Watson Research Center, Yorktown Heights, New York 10598*

(Received 11 June 1973)

Near-resonant light pulses were steepened by passage through Rb vapor. The rise time changed from typically 4 nsec to less than 1 nsec, and complicated envelopes developed. The self-steepening, well described by adiabatic following, results from (i) an intensity-dependent pulse velocity, (ii) self-phase modulation combined with strong group-velocity dispersion. Numerical integration gives quantitative agreement with observations and indicates shock formation on the leading edge.

The possibility of observing self-steepening of optical pulses and the formation of shocks has been extensively discussed.<sup>1-9</sup> An early problem was that of pulse propagation in a medium with an intensity-dependent refractive index but no dispersion.<sup>2,3</sup> The resulting pulse reshaping is entirely caused by the intensity-dependent pulse velocity. This steepening effect has remained unobserved because either the propagation distances and input powers required are unattainable, or

dispersion cannot be rightly neglected. With dispersion included in the analysis,<sup>1,4,7,8</sup> self-steepening was predicted to occur over much shorter distances. It is then mainly caused by self-phase modulation, which modifies the instantaneous frequency along the pulse, thereby producing reshaping due to group-velocity dispersion. Even though the conditions required to observe this type of self-steepening are more favorable, experimental verification has not been obtained.

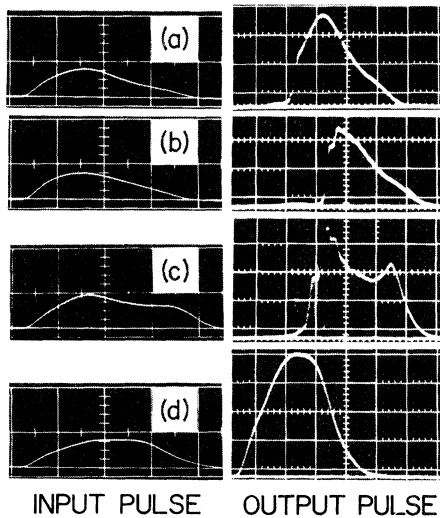


FIG. 1. Input pulses (300 W/large division  $\times$  5 nsec/large division) to the 100-cm Rb cell and the resulting output (5 nsec/large division). The relative intensity scale is the same for all the output pulses. The detectors were ITT biplanar photodiodes; the input was observed with a Tektronix 519 oscilloscope, which triggered a Tektronix 7904 oscilloscope monitoring the output. (a)  $(\nu_0 - \nu)/c = 0.24 \text{ cm}^{-1}$ , where  $\nu_0$  is the center frequency of the Rb line (7948 Å) and  $\nu$  is the input frequency. (b)  $(\nu_0 - \nu)/c = 0.20 \text{ cm}^{-1}$ . (c)  $(\nu_0 - \nu)/c = 0.23 \text{ cm}^{-1}$ . (d)  $(\nu_0 - \nu)/c = 0.78 \text{ cm}^{-1}$ .

We report what is believed to be the first direct observation of self-steepening of optical pulses caused by a nonlinear electric susceptibility. Our results are different in kind from pulse compression obtained for self-induced transparency with converging beams.<sup>10,11</sup> The experiment used the strong, near-resonant nonlinearity of an alkali vapor.<sup>5,7,9,12,13</sup> This nonlinearity is many orders of magnitude larger than that of the usually discussed Kerr liquids. Excellent agreement is obtained between experiment and theory. The latter includes the related effects of intensity-dependent pulse velocity, self-phase modulation, and linear plus nonlinear dispersion.

Short pulses of narrow-line, circularly polarized, dye-laser light on the low-frequency side of the Zeeman-split  $^2P_{1/2}$  resonance line of Rb (7948 Å) were passed through dilute Rb vapor. Figure 1 shows examples of reshaping; self-steepening is manifested by an abrupt discontinuity on the leading edge of the output pulse [Figs. 1(a) and 1(b)]. The observed 1-nsec rise time is that of the detection system. More intense, or more nearly resonant, pulses develop complicated envelopes with abrupt rises and multiple

peaks [Fig. 1(c)]. The pulse of Fig. 1(d) is far off resonance, shows little reshaping or attenuation, and propagates with a group velocity of  $0.8c$ . Comparing the pulses of Fig. 1(a)–1(c) with Fig. 1(d), one determines their velocity  $\lesssim c/4$  and their attenuation  $\lesssim 30\%$ .

The experimental arrangement, described elsewhere,<sup>9</sup> is modified as follows. The dye-laser beam illuminates a 1-mm aperture and travels to a  $f = -103 \text{ cm}$  lens positioned 525 cm away from the aperture; 20 cm beyond the lens the pulse enters the cell. The beam profile at the lens is the Fraunhofer diffraction pattern of the aperture. The negative lens changes the radius of the spherical wave from 525 to 86 cm at the lens position. This reduces self-defocusing<sup>13</sup> to a negligible value; no change in the beam profile could be observed. An additional Fabry-Perot interferometer with a resolution of  $0.01 \text{ cm}^{-1}$  monitors the spectrum of the reshaped pulse. Finally, the output window of the cell is imaged with unit magnification on a 3-mm aperture placed in front of the output photodiode. As previously, the Rb cell is in an axial magnetic field of about 10 kG; the cell temperature is  $120^\circ\text{C}$ , corresponding to an atomic number density of  $1.8 \times 10^{13}/\text{cm}^3$ . The linewidth of the input light is  $0.003 \text{ cm}^{-1}$ . The photodiodes are calibrated against a TRG thermopile.

For the regime studied here the nonlinear response is well described by adiabatic following,<sup>9,12,13</sup> in which the pseudomoments of the atoms remain closely aligned with the changing effective field of the pulse. Since the group velocity is exceptionally dispersive it is essential to account for the change in instantaneous frequency caused by self-phase modulation. The Bloch equations describing a two-level system of resonant frequency  $\omega_0$  in a frame rotating at the instantaneous field frequency  $\omega + \partial\varphi/\partial t$  are well known. The equations are written in terms of the Rabi precession angular frequency  $\mathcal{E} = \sqrt{2}p_{12}E/\hbar$  and the angular frequency offset  $\gamma = \omega_0 - \omega - \partial\varphi/\partial t$ . Here  $E$  and  $\varphi$  are the slowly varying field envelope and phase, respectively;  $p_{12}$  is the magnitude of the  $\sigma$  dipole matrix element. The in-phase and out-of-phase components of the polarization are  $u$  and  $v$ , respectively;  $W$  is the atomic energy density.<sup>10</sup> Within the adiabatic-following approximation these quantities are obtained from the vector model.<sup>9</sup> Formally the approximation consists in setting  $\partial v/\partial t = 0$  in the equation  $\partial v/\partial t = -u\gamma - \sqrt{2} \times p_{12} \mathcal{E} W / (\hbar \omega_0)$ . An expression for  $u$  results which is used in  $\partial u/\partial t = v\gamma - u/T_2$  to give  $v$ . The small-

ness of the resulting  $\partial v/\partial t$  compared to  $u\gamma$  justifies the procedure. In the absence of relaxation the equation  $\partial W/\partial t = v\mathcal{E}\hbar\omega_0/(\sqrt{2}p_{12})$  is then integrated exactly, giving  $W = -\frac{1}{2}\hbar\omega_0 N_e(1 + \mathcal{E}^2/\gamma^2)^{-1/2}$ , where  $N_e$  is the effective atomic number density. With moderate relaxation this relation holds approximately.

These results are introduced in the coupled, reduced wave equations<sup>14</sup>

$$c \partial E/\partial z + \partial E/\partial t = -2\pi\omega v, \quad (1a)$$

$$c \partial \varphi/\partial z + \partial \varphi/\partial t = -2\pi\omega u/E. \quad (1b)$$

Equation (1a) and the time partial derivative of (1b) are recast in terms of  $\mathcal{E}$  and  $\gamma$ . The final equations are written in terms of an initial constant offset  $\gamma = \delta$ , a coupling strength  $S = 2\pi N_e \omega p_{12}^2/(\hbar\delta^2)$ , a normalized distance  $\xi = z/c$ , and a local time  $\tau = t - z/v_g$ . The group velocity at low intensities,<sup>9</sup> valid for  $\mathcal{E}$  and  $\gamma$ , is  $v_g = c/(1+S)$  provided  $\delta \ll \omega$ . With  $T_2 = \infty$  the equations are

$$\partial \mathcal{E}/\partial \xi = M \partial \mathcal{E}/\partial \tau + N \mathcal{E} \partial \gamma/\partial \tau, \quad (2a)$$

$$\partial \gamma/\partial \xi = M \partial \gamma/\partial \tau - N \mathcal{E} \partial \mathcal{E}/\partial \tau, \quad (2b)$$

where  $M = S[1 - (\delta/\gamma)^2(1 + \mathcal{E}^2/\gamma^2)^{-3/2}]$  and  $N = S\delta^2\gamma^{-3} \times (1 + \mathcal{E}^2/\gamma^2)^{-3/2}$ . The terms in  $M$  account for the intensity and frequency dependences of the pulse velocity. These constitute one steepening mechanism. The term in  $N$  in Eq. (2a) describes nonlinear dispersion. For small  $\mathcal{E}$  it becomes identical to the usual result of linear dispersion theory. The term in  $N$  in Eq. (2b) describes self-phase modulation. The combination of dispersion and self-phase modulation is another steepening mechanism. Under present experimental conditions both mechanisms contribute to the final pulse shape, the second being the stronger. The self-steepening is identical on both sides of the resonance line since (2) is unchanged when  $\gamma$  changes sign.

The discriminant of this system of coupled partial differential equations is  $\Delta = -2M - 4(M^2 + \mathcal{E}^2 N^2)$ , which is usually negative. The system is therefore elliptic, though the boundary conditions (specification of  $\mathcal{E}$  and  $\gamma$  for all  $\tau$  at the cell entrance) are appropriate to a hyperbolic problem. Such improperly posed elliptic problems lead to singular solutions.<sup>6,15</sup> Both analytical results<sup>6,15</sup> and numerical integration show that irregularities in the input grow rapidly, as demonstrated by Figs. 1(a) and 1(c). The input pulse [Fig. 1(c)] has slightly more structure, is slightly closer to the line, and is 20% more powerful than the input 1(a). These small differences cause the ex-

treme difference between the outputs, where tiny features on the input 1(c) are changed to dramatic structure.

As a steep front forms, the adiabatic-following approximation will break down and additional terms are required to describe the polarization. These determine the sharpness of the front and its evolution. Such terms should also allow for steady-state solutions  $\mathcal{E} = \mathcal{E}(\tau - a\xi)$  and  $\gamma = \gamma(\tau - a\xi)$ . Equations (2) do not admit such solutions. In particular the  $2\pi$  sech pulses of self-induced transparency do not, strictly speaking, satisfy the equations. However, it has been found both experimentally and numerically that any pulse for which  $\mathcal{E}$  is much smaller than  $\delta$  experiences no measureable reshaping or frequency modulation over the propagation distances considered here. Off-resonance sech pulses as described by Diels and Hahn<sup>16</sup> evolve over much longer distances than are of interest in the present experiment. As seen below, Eqs. (2) describe appropriately the strong reshaping of pulses for which  $\mathcal{E}$  approaches  $\delta$ .

In order to compare theory and experiment it is necessary to account for the ten hyperfine components ( $\omega_{0i}$ ,  $i = 1$  to 10) of the Rb line, for the diffraction of the spherical wave, and for the absorption caused by  $T_2$ . One defines ten coupling strengths  $S_i$ , ten offsets  $\gamma_i = \Gamma + \delta_i$ , where  $\Gamma = -\partial\varphi/\partial t$ , and the group velocity  $v_g = c/(1 + \sum_i S_i)$ . Equations (2) are replaced by

$$\begin{aligned} \partial \mathcal{E}/\partial \xi = m \partial \mathcal{E}/\partial \tau + n \mathcal{E} \partial \Gamma/\partial \tau \\ - \mathcal{E}/(\xi_0 + \xi) - c\alpha\mathcal{E}/2, \end{aligned} \quad (3a)$$

$$\partial \Gamma/\partial \xi = m \partial \Gamma/\partial \tau - n \mathcal{E} \partial \mathcal{E}/\partial \tau, \quad (3b)$$

where  $m$  and  $n$  are sums over ten terms similar to  $M$  and  $N$ ,  $\xi_0$  is the time of travel from the center of the spherical wave to the cell entrance at  $\xi = 0$ , and

$$\alpha = 2(cT_2)^{-1} \sum_i S_i \delta_i^2 \gamma_i^{-2} (1 + \mathcal{E}^2/\gamma_i^2)^{-1/2}$$

is the nonlinear absorption coefficient.

Figure 2 shows the result of applying Eqs. (3) to the input pulse of Fig. 1(a). The stability of the numerical integration requires that the input be a function with continuous derivatives. This pulse fits a ninth-degree polynomial with a relative rms deviation of 0.002. For comparison to the output (solid line), the input pulse (dashed line) has been drawn as if it had gone through the cell at the group velocity subject only to linear absorption and diffraction. With this normalization, and except for the intensity dependence of

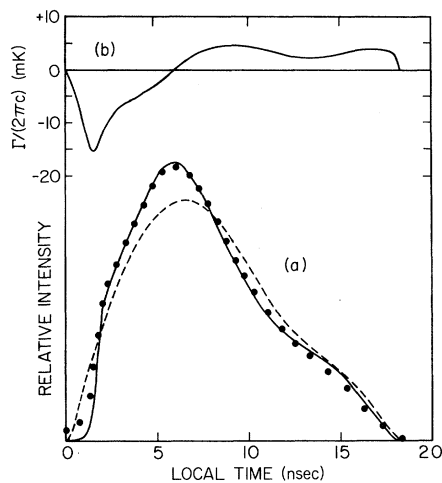


FIG. 2. The output pulse (dots) of Fig. 1(a) compared with the calculated pulse (solid line) and the normalized input (dashed line). (b) Calculated self-phase modulation  $\Gamma = \partial\phi/\partial t$  in  $10^{-3} \text{ cm}^{-1}$ .

$\alpha$ , the energies of the input and output pulses are equal. In particular the output peak is higher than the input because of the time compression, in good agreement with the calibration deduced from Fig. 1(d). The calculated output agrees remarkably well with the measured points. The integration indicates that the leading edge of the pulse was still steepening at the end of the cell. Figure 2(b) shows that the predicted self-phase modulation is proportional to the time derivative of  $\mathcal{E}^2$  in conformity with (3b). Its extent is of the order of the resolution of the output interferometer, and indeed broadening could not be clearly observed. All parameters of the calculation are experimentally measured. The input power was adjusted to 170 W, while the measured value was 200 W; this is within the accuracy of the calibration. The adjusted power corresponds to a peak input intensity of  $500 \text{ W/cm}^2$ , a pulse area<sup>10</sup>  $\approx 40\pi$ , and a maximum  $\mathcal{E} \approx 0.06 \text{ cm}^{-1}$ . The excellent agreement between experiment and theory for this and other similar pulses shows that the adiabatic-following approximation is valid during reshaping.

In Fig. 1(b) the measured 1-nsec output rise time is that of the oscilloscope. Some spectral broadening mostly to the high-frequency side, as predicted, was observed. Numerical integration of this pulse produces a steep front 30 cm before

the output window; the integration of (3) cannot be continued beyond this point. The fact that a rise-time-limited leading edge is still obtained at the output strongly suggests that a shock traveled the remaining 30 cm. By shock we mean an extremely sharp front propagating with little reshaping, because of dynamic balance between the steepening mechanisms of Eqs. (3) and a smoothing mechanism, not taken into account in (3) and operating only during extremely rapid variations of the field. This will be the subject of further investigations.

The authors would like to acknowledge useful discussions with P. D. Gerber, R. Landauer, and Michael M. T. Loy. The skilled technical assistance of R. J. Bennett was essential to this work.

\*Work was partially supported by the U. S. Office of Naval Research under Contract No. N00014-70-C-0187.  
 †Permanent address: IBM Zurich Research Laboratory, 8803 Rüschlikon, Switzerland.

<sup>1</sup>L. A. Ostrovskii, Zh. Eksp. Teor. Fiz. **51**, 1189 (1966) [Sov. Phys. JETP **24**, 797 (1967)].

<sup>2</sup>R. J. Joenk and R. Landauer, Phys. Lett. **24A**, 228 (1967).

<sup>3</sup>F. DeMartini, C. H. Townes, T. K. Gustafson, and P. L. Kelley, Phys. Rev. **164**, 312 (1967).

<sup>4</sup>T. K. Gustafson, J. P. Taran, H. A. Haus, J. R. Lifshitz, and P. L. Kelley, Phys. Rev. **177**, 306 (1969).

<sup>5</sup>V. M. Arutyunyan, N. N. Badalyan, V. A. Iradyan, and M. E. Movsesyan, Zh. Eksp. Teor. Fiz. **58**, 37 (1970) [Sov. Phys. JETP **31**, 22 (1970)].

<sup>6</sup>B. B. Kadomtsev and V. I. Karpman, Usp. Fiz. Nauk **103**, 193 (1971) [Sov. Phys. Usp. **14**, 40 (1971)].

<sup>7</sup>B. Ya. Zel'dovich and I. I. Sobel'man, Pis'ma Zh. Eksp. Teor. Fiz. **13**, 182 (1971) [JETP Lett. **13**, 129 (1971)].

<sup>8</sup>F. Shimizu, IEEE J. Quantum Electron. **8**, 851 (1972).

<sup>9</sup>D. Grischkowsky, Phys. Rev. A **7**, 2096 (1973).

<sup>10</sup>S. L. McCall and E. L. Hahn, Phys. Rev. **183**, 457 (1969).

<sup>11</sup>H. M. Gibbs and R. E. Slusher, Appl. Phys. Lett. **18**, 505 (1971).

<sup>12</sup>D. Grischkowsky, Phys. Rev. Lett. **24**, 866 (1970).

<sup>13</sup>D. Grischkowsky and J. A. Armstrong, Phys. Rev. A **6**, 1566 (1972).

<sup>14</sup>In (1) the linear index of refraction  $n_0$  is set equal to unity since  $(n_0 - 1) < 10^{-4}$ .

<sup>15</sup>M. J. Lighthill, Proc. Roy. Soc., Ser. A **299**, 28 (1967).

<sup>16</sup>J. C. Diels and E. L. Hahn, Phys. Rev. A (to be published).

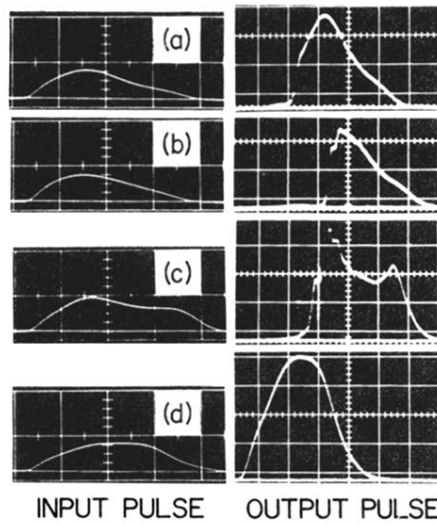


FIG. 1. Input pulses ( $300 \text{ W}/\text{large division} \times 5 \text{ nsec}/\text{large division}$ ) to the 100-cm Rb cell and the resulting output ( $5 \text{ nsec}/\text{large division}$ ). The relative intensity scale is the same for all the output pulses. The detectors were IIT biplanar photodiodes; the input was observed with a Tektronix 519 oscilloscope, which triggered a Tektronix 7904 oscilloscope monitoring the output. (a)  $(\nu_0 - \nu)/c = 0.24 \text{ cm}^{-1}$ , where  $\nu_0$  is the center frequency of the Rb line ( $7948 \text{ \AA}$ ) and  $\nu$  is the input frequency. (b)  $(\nu_0 - \nu)/c = 0.20 \text{ cm}^{-1}$ . (c)  $(\nu_0 - \nu)/c = 0.23 \text{ cm}^{-1}$ . (d)  $(\nu_0 - \nu)/c = 0.78 \text{ cm}^{-1}$ .